Terahertz emission spectroscopy of ultrafast exciton shift current in the noncentrosymmetric semiconductor CdS

M. Sotome, M. Nakamura, T. Morimoto, Y. Zhang, G.-Y. Guo, M. Kawasaki, N. Nagaosa, Y. Tokura, and N. Ogawa

Phys. Rev. B **103**, L241111 — Published 21 June 2021

DOI: 10.1103/PhysRevB.103.L241111

Terahertz emission spectroscopy of ultrafast exciton shift-current in non-centrosymmetric semiconductor CdS

M. Sotome[1]*, M. Nakamura[1,2], T. Morimoto[2,3], Y. Zhang[4], G.-Y. Guo[1,5,6], M. Kawasaki[1,3], N. Nagaosa[1,3], Y. Tokura[1,3,7] and N. Ogawa[1,2,3]

[1]RIKEN Center for Emergent Matter Science (CEMS), Wako, 351-0198, Japan

[2]PRESTO, Japan Science and Technology Agency (JST), Kawaguchi 332-0012, Japan

[3]Department of Applied Physics and Quantum-Phase Electronics Center (QPEC), University of Tokyo, Tokyo, 113-8656, Japan

[4]Department of Physics, Massachusetts Institute of Technology, Cambridge, Massachusetts 02139, USA

[5]Department of Physics, National Taiwan University, Taipei 10617, Taiwan

[6]Physics Division, National Center for Theoretical Sciences, Hsinchu 30013, Taiwan

[7]Tokyo College, University of Tokyo, Tokyo 113-8656, Japan

*To whom correspondence may be addressed. Email: masato.sotome@riken.jp

PACS:

71.35.−y (Excitons and related phenomena),

72.40.+w (Photovoltaic effect in bulk matter),

78.47.D- (Picosecond techniques in spectroscopy of solid state dynamics),

88.40.H- (Solar cells).

Abstract

Charge-neutral exciton has been predicted to carry genuine photocurrent due to the geometric Berry phase of the electronic bands, if the inversion symmetry in a crystal is broken. We detect such exciton shift-current in a prototypical polar semiconductor CdS by using terahertz emission spectroscopy. A distinct peak emerges in the photocurrent spectra at the energy of the exciton resonance, which is demonstrated to result from the distinct displacements of electrons and holes in real space within the excitons to produce a finite transient charge current at sub-picosecond time scale. Our findings elucidate the Berry phase physics of the charge-neutral photoexcitations and also shed light on the novel energy harvesting mechanism by exciton generation.

Main text

An exciton is a bound pair of an electron and a hole attracted by the Coulomb potential, which is charge neutral. Since the exciton gains energy electrostatically, photons with the energy below the bandgap can be absorbed upon exciton formation. The energy E_{ex} measured from the bandgap is the exciton binding energy, corresponding to this Coulombic energy gain. For the optical excitation in solids, these excitons always play important roles. For example, in conventional photodetectors or in solar cells, the excitons are created at the first stage, and then separated by the internal/external electric-field to promote charge currents into the electrodes. For the real application, a variety of excitonic processes, including multiple exciton generation, have been employed. Although the exciton itself is charge neutral, it is predicted recently that the process of exciton formation actually accompanies photocurrent by the shift-current mechanism [1, 2]. The shift current arises from an instantaneous spatial shift of electron (hole) cloud in

real space upon photoexcitation [3-5], driven by the geometrical character (Berry connection) of the constituting electron bands.

The wave functions of the electron and the hole in a noncenctrosymmetric crystal shift in real space when forming exciton. Therefore, excitation of such exciton also supports circuit photocurrent, even without electric or thermal separation of exciton [Figs. 1(a),(b)]. The amplitude of the exciton shift-current is expected to be comparable to or slightly smaller than that of the above-bandgap quasiparticle excitation, since the charge shift can be reduced due to their bound character [1, 6].

There are three key requirements to observe exciton shift-current in real material [1]: (i) In the excitation spectrum, the exciton absorption should be well separated from the conduction band continuum. (ii) The system should be cooled to reduce thermal separation of exciton into free carriers. (iii) The photoexcitation should be distant from electrodes to avoid extrinsic effects, such as the charge accumulation at the semiconductor/metal junctions.

Photocurrent generation at the time-scale of elementary optical-transition process can be studied by using terahertz (THz) optics without electrodes [7]. When detecting photocurrent by conventional electric circuits, we often suffer from current artifacts from electrode contacts, insufficient temporal response of preamplifiers, etc. On the contrary, if we measure electromagnetic wave radiated from a transient photocurrent, which is in the THz frequency in many cases, we can retrieve the ultrafast charge dynamics in a non-contact manner, at the spatial resolution of incident laser spot.

Some THz experiments on the ultrafast photocurrent (and shift current) have been reported on III-V semiconductor bulk crystals [8], semiconductor superlattices [9, 10], semiconductor nanosheets [11], ferroelectric semiconductors [12, 13], topological

insulators [7], and Weyl semimetals [14-16]. In reality, the ultrafast THz photocarrier dynamics in GaAs/InGaAs quantum-well [17, 18] have shown enhanced responses at the exciton resonance. However, these experiments were performed at room temperature where the exciton and above-bandgap transitions are hardly separable, and have not been discussed in the light of the exciton shift-current.

In this Letter, we demonstrate the presence of exciton shift-current in a CdS crystal at low temperature (2 K) by utilizing THz emission spectroscopy. Femtosecond optical excitation at the exciton resonance was found to generate sizable transient shift-current, leading to the electromagnetic radiation into the free space. We analyze this radiation in detail with varying the incident photon energy and intensity.

CdS has a non-centrosymmetric polar wurtzite structure with a direct bandgap in the visible energy range (2584 meV at 2 K) and with relatively large exciton binding energy E_{ex} of ~30 meV [19-22]. It has long been used as commercial photoresistors. CdS is also known to show a quantum-mechanical interference in the photocurrent [23] and has been a target material to demonstrate the existence of shift-current under the above-bandgap photoexcitation [4, 24]. We used 1-mm-thick 5 x 5 mm^2 CdS$(1\bar{1}00)$ crystals with high resistivity with resistivity of $1 \times 10^{11}\ \Omega \cdot \mathrm{cm}$ (SurfaceNet GmbH, Germany). The crystal was optically polished, etched in HCl solution, and subsequently cooled to 2 K in helium atmosphere. A Ti:sapphire regenerative amplifier (130 fs at 1 kHz) and an optical parametric amplifier are employed for excitation. The spectral width of the laser pulse was 28 meV (full width at half maximum, HWHM) when without further treatments. The THz radiation from the excitation spot in the reflection geometry was focused on a 2-mm-thick ZnTe(110) and measured by electro-optical sampling [12, 25].

In bulk crystals lacking inversion symmetry, spontaneous photocurrent J has two

contributions as $J = J_{\mathrm{con}} + J_{\mathrm{ex}}$, where J_{con} is the conventional shift-current with the above-bandgap excitation and J_{ex} is the exciton shift-current [Fig. 1(b)]. These two contributions can be expressed as [1]

$$J_{\mathrm{con}}(\omega) = \frac{e^3}{\hbar^2}\left|\frac{E_{\mathrm{laser}}}{\omega}\right|^2 \int \frac{dk^3}{(2\pi)^3}|v_{12}(k)|^2 R(k)\ \frac{\Gamma}{\left(\omega-\omega_{\mathrm{cv}}(k)\right)^2+\Gamma^2}. \qquad (1)$$

$$J_{\mathrm{ex}}(\omega) = \frac{2e^3}{\hbar^2}\left|\frac{E_{\mathrm{laser}}}{\omega}\right|^2 (\delta k)^3|v_{12}(0)|^2 R(0)\ \frac{\Gamma}{(\omega-\omega_{\mathrm{ex}})^2+\Gamma^2}. \qquad (2)$$

Here, E_{laser} is the electric field of incident laser with angular frequency ω, $\hbar\omega_{\mathrm{cv}}(\boldsymbol{k}) = E_{\mathrm{c}}(\boldsymbol{k}) - E_{\mathrm{v}}(\boldsymbol{k})$ is the energy difference between the valence and conduction electrons with $E_{\mathrm{c}}(\boldsymbol{k})$ [$E_{\mathrm{v}}(\boldsymbol{k})$] the conduction (valence) band dispersion, $v_{12}(\boldsymbol{k}) = \langle \psi_{\mathrm{v},k} \ |\hat{v}|\psi_{\mathrm{c},k} \rangle$ the interband matrix element of the velocity operator $\hat{v}$ with $\psi_{\mathrm{c/v}}$ being the wave-function for the conduction/valence band, $R = \frac{\partial}{\partial k_j}\mathrm{Im}[\log v_{12}] + a_1 - a_2$ the shift vector, and Γ the scattering rate of the electron-hole pair. $\hbar\omega_{\mathrm{ex}}$ is the energy of exciton excitation, and $(\delta k)^3$ is the small volume in the Brillouin zone within the energy range of exciton binding energy above the band gap, where the Bloch states participate in the exciton formation. (We assume that the band gap is located at $\boldsymbol{k}$ = 0.) We find that J_{con} is non-zero only for the photon energy $\hbar\omega$ exceeding the bandgap. In contrast, the J_{ex} is nonzero at the exciton absorption at $\hbar\omega_{\mathrm{ex}}$ below the band gap [Fig. 1(b)]. We note that the above exciton shift current formula applies for shallow, i.e. small-E_{ex}, excitons where the exciton is formed by Bloch states near the band gap [Supplemental Material [26]]. The formula for general cases can be found in Ref. 1.

Figure 1(c) shows the representative THz waveforms at several excitation photon energies. Here the excitation at 2552 meV is resonant with the exciton absorption in CdS at 2 K as will be discussed later [39]. Note that there exist three exciton resonances in CdS derived from three valence bands near the Γ-point (named *A*-, *B*-, and *C*-exciton see

Fig. 1(a)). The *C*-exciton absorption is located higher than the band-edge (Fig. 1(a)) [40]. In principle, *A*-exciton (A_{ex} in Fig. 1(a)) photoabsorption is forbidden [19] in our setup ($E_{\mathrm{laser}} \parallel c$ or $E_{\mathrm{laser}} \perp c$, where E_{laser} indicates the electric field of incident laser, with detected radiation $E_{\mathrm{THz}} \parallel c$). However, the magnetic field of light or finite momentum of photon is known to realize the *A*-exciton (n = 1) absorption [19, 41]. Previous studies also revealed the photocurrent generation at the *A*-exciton resonance under the electric bias [42, 43], in which photoexcited exciton-polaritons are forced to separate into free carriers.

We find a clear difference in the peak positions (by ~0.25 ps) in the THz waveforms for the below-bandgap ($\hbar\omega$ = 2480 meV) and above-bandgap ($\hbar\omega \geq$ 2580 meV) excitations, corresponding to nearly $\pi/2$ phase shift for the central frequency (~1.0 THz). This phase shift manifests the difference in the origin of THz emission; shift current by the above-bandgap and the optical rectification (OR) by the below-bandgap photoexcitation [4, 44]. The spectrum at the exciton resonance ($\hbar\omega$ = 2552 meV) seems to be a mixture of two features. We have performed factor analysis, which can search the base waveforms and their relative contributions from possibly mixed signals [45]. This technique is well-known in the analysis of photo luminescence spectra for the molecular species identification [46]. As a result of this analysis, we separated the THz waveforms into two distinct origins [Fig. 1(d)] [12, 13].

In Fig. 2(a), we plot the second-order photoconductivity $\sigma^{(2)}_{ccc}$ spectrum deduced via the factor analysis [Supplemental Material [26]]. A peak at the *A* exciton resonance (2552 meV) is discerned in the spectrum of the shift-current, whereas no corresponding feature for the in-gap OR. The in-gap OR component shows phase reversal (being positive to negative in sign) at the bandgap energy, in agreement with the reported first principles

calculations [4]. We evaluate the shift distance $r_{\mathrm{shift}} = 0.12\ \AA$ ($\sigma^{(2)}_{ccc} = 0.17\ \mu\mathrm{A/V^2}$) at the exciton resonance by comparing the amplitude of emitted THz wave with that from (110) ZnTe, while that for the above-bandgap excitation (at 2612 meV) is found to be $r_{\mathrm{shift}} = 0.21\ \AA$ ($\sigma^{(2)}_{ccc} = 0.30\ \mu\mathrm{A/V^2}$). These numbers are somewhat smaller compared to those in the previous first-principles calculations [4]. Our first-principles calculation for J_{con}, incorporating the spin-orbit interaction (SOC) but without excitonic effects, is found to show a comparable amplitude with our experimental spectrum (Fig. 2(a), see Supplementary Material for detail). Generally, the nonlinear optical conductivity $\sigma^{(2)}_{ccc}$ between the band-edge and the exciton resonance energy will be renormalized with the existence of exitonic interactions, as seen in the experimental data. Note that it is difficult to incorporate the excitonic effects to the first-principles calculation used here. The absolute value of the $\sigma^{(2)}_{ccc}$ is smaller than the previous report on the THz emission experiments excited above the bandgap energy ($r_{\mathrm{shift}} = 2\ \AA$, and $\sigma^{(2)}_{ccc} = 6\ \mu\mathrm{A/V^2}$ at 3000 meV) [24]. This discrepancy may come from the large difference in the absorption coefficient α_{laser} at the photon energy used, since $\sigma^{(2)}$ is proportional to $r_{\mathrm{shift}}\alpha_{\mathrm{laser}}$ [24].

We fit the second-order photoconductivity spectrum by four Lorentz peaks (one being for the exciton resonance and the higher-lying three for the phenomenological representation of the continuous electron-hole excitations derived from three valence bands, Fig. 1(a)) convoluted with the gaussian laser spectrum (FWHM of 28 meV) as shown in Fig. 2(a);

$$\sigma_{\mathrm{exp}}(\omega) = \frac{1}{\sqrt{2\pi}\sigma_{\mathrm{laser}}}\exp\left(-\frac{\omega^2}{2\sigma^2_{\mathrm{laser}}}\right) * \ \mathrm{Re}\left[\sum_{i=1,2,3,4}\frac{\sigma_i}{\hbar^2(\omega^2-\omega_i^2+2i\gamma_i\omega_i)}\right]. \quad (3)$$

The lowest energy peak was found to have the resonance energy $\epsilon_1 = \hbar\omega_1 = 2550\pm2$ meV and scattering parameter $\hbar\gamma_1 = 7.7 \pm 3.2$ meV. These are in good agreement with the *A*

exciton parameters in CdS reported in previous studies; ϵ_1 = 2552 meV for the absorption [40] and dielectric spectrum at 2 K [47], and □γ = 7.8 meV in the electric-field modulation reflectance spectroscopy at 13 K [48]. From an order-of-magnitude estimation by using Eqs. (1) and (2), the amplitude of the exciton shift current J_{ex} is expected to be comparable to that for the above-bandgap shift current J_{con} integrated over the energy range of exciton binding energy from the absorption edge. Our fitting is consistent with this prediction, supporting the existence of the exciton shift current. For the incident laser polarization normal to the *c*-axis ($E_{\mathrm{laser}} \perp c$), the shift-current spectrum shows the exciton resonance ~2 meV lower compared with that for $E_{\mathrm{laser}} \parallel c$ [See Supplemental Material [26]]. This difference is ascribed to the excitation of longitudinal-transverse (LT)-mixed mode in CdS, from the analyses of polarization dependent absorption spectra [34-36]. The L-T splitting of *A*-exciton energy was reported to be 1.9 meV [49, 50]. The overall fitting parameters can be found in the Supplemental Material [26].

The spectrum in Fig. 2(a) is evaluated with considering the incident laser spectral width (FWHM) of $2\sqrt{2\ln 2}\sigma_{\mathrm{laser}} = 28$ meV, which is rather comparable to the exciton binding energy (30 meV) of CdS. To confirm the presence of exciton shift-current, we repeated the measurements by modifying the spectral width of the incident laser by using a monochromator (FWHM $2\sqrt{2\ln 2}\sigma_{\mathrm{laser}}^{\mathrm{narrow}}$ to be 15 meV). The resultant THz amplitude spectrum is shown in Fig. 2(b). We fit the spectrum without the factor analysis for this case, which again revealed a distinct peak at the exciton resonance. The narrow bandwidth excitation made the *A*-exciton peak more pronounced.

Other nonlinear optical effects resonant with the exciton may show a similar incident photon energy dependence. We calculate the photocurrent dynamics $J(t)$ [Fig. 3(a)] [12, 13, 26]. The time-domain dynamics was fitted by the following formula [solid

lines in Fig. 3(a)];

$$J(t) = \frac{1}{\sqrt{2\pi}\tau_{\mathrm{r}}} \exp\left(\frac{-t^2}{2\tau_{\mathrm{r}}^2}\right) * \left[J_{\mathrm{shift}}\delta(t) - J_{\mathrm{decay}}u(t)\exp\left(-\frac{t}{T}\right)\right], \quad (4)$$

where the asterisk operator $(*)$ means the convolution, τ_{r} is the instrumental time resolution ($\sim$0.28 ps), J_{shift} amplitude of shift-current, and J_{decay} partial relaxation of shift with a decay time T. Here the negative sign on J_{decay} (current in opposite direction) indicates that the electrons' and holes' spatial-shift is randomized to some extent on this time scale [51], leading to reversal flow of the charge current [3]. Fitting analysis of $J(t)$ dynamics by eq. (4) has been reported previously in topological insulators [7] and ferroelectric semiconductors [12, 13]. Optical transitions play predominant role in the first term of eq. (4) [J_{shift}], and the decoherence processes should be the origin of the second term [J_{decay}] (Refs. 7, 52-54).

Figure 3(c) shows the incident photon energy dependence of the scattering rate $1/T$. We obtained $T = 0.32$ ps (2556 meV), for which $\hbar/T = 13$ meV is in good agreement with the half linewidth of the exciton absorption ($\hbar/T = 10$ meV) in CdS. The longer T for the lower photon energy excitation below the *A*-exciton resonance (2540 meV, red line) should be ascribed to the smaller excess energy at the exciton generation, or excitation of a different polariton branch, which is omitted in Fig. 1(a) for simplicity. For the excitation above the bandgap, *T* is found to be about 0.4 ps ($1/T = 2.5$ THz). Previous studies have discussed the damping of excitonic polaritons considering the couplings with optical and acoustic phonons [55, 56].

The incident laser power dependence for the in-gap excitation (2480 meV) reveals that the square root of the THz intensity (I_{THz}) increases linearly ($I_{\mathrm{THz}}^{1/2} \propto |E_{\mathrm{laser}}|^2 \propto I_{\mathrm{laser}}$) [Fig. 4(a)], which is consistent with the process expected for the in-gap OR ($E_{\mathrm{OR}} \propto P_{\mathrm{OR}} \propto {E_{\mathrm{laser}}}^2 \propto I_{\mathrm{laser}}$) [13]. In stark contrast, we confirmed that the THz

intensity shows the crossover from linear to sub-linear behavior as the laser intensity increases for the exciton and above-bandgap excitations [Figs. 4(b) to (d)], which is a hallmark of the shift-current [57],

$$I_{\mathrm{THz}}^{1/2} \propto j_{\mathrm{shift}} \propto \frac{\frac{\Gamma}{2}|E_{\mathrm{laser}}|^2}{\sqrt{(\frac{e\ v_{12}\ |E_{\mathrm{laser}}|}{\hbar\omega})^2 + \left(\frac{\Gamma}{2}\right)^2}}. \qquad (5)$$

This crossover behavior from $|E_{\mathrm{laser}}|^2$ to $|E_{\mathrm{laser}}|$ arises from the increase of stimulated radiation from the excited state for higher power. All the above observations point to the emergence of exciton shift-current in CdS.

In summary, we have experimentally demonstrated the existence of exciton shift-current in CdS as measured by THz emission spectroscopy. The photocurrent dynamics, as exemplified in the emitted THz waveforms, changes from the conventional in-gap optical rectification to the real excitation at the exciton resonance (and also for the above-bandgap excitation) while varying the photon energy. The incident power dependence also supports the presence of the exciton shift-current. Thus, it is concluded that the charge-neutral exciton can support transient photocurrent through the shift-current mechanism. In materials with high covalency including many photovoltaic materials, the photoexcited state has excitonic characters [58]. Our results suggest future applications of exciton excitation in energy harvesting devices, especially in organic semiconductor and hybrid organic-inorganic perovskites.

Acknowledgement

This research is supported by JSPS KAKENHI Grant Numbers 18K14155, 17H02914,

and 18H03676. M.N., T.M. and N.O. are supported by PRESTO, JST (JPMJPR16R5, JPMJPR19L9, JPMJPR17I3, respectively). TM is supported by JST CREST (JPMJCR19T3). NN is supported by JST CREST Grant Number JPMJCR16F1. YZ is supported by the DOE Office of Basic Energy Sciences under Award desc0018945 to Liang Fu.

References

[1] T. Morimoto and N. Nagaosa, Phys. Rev. B **94**, 035117 (2016).

[2] Y.-H. Chan, Diana Y. Qiu, Felipe H. da Jornada, and Steven G. Louie, arXiv:1904.12813v1, posted 29 Apr 2019 (2019).

[3] R. von Baltz and W. Kraut, Phys Rev B **23**, 5590 (1981).

[4] J. E. Sipe and A. I. Shkrebtii, Phys. Rev. B **61**, 5337 (2000).

[5] S. M. Young and A. M. Rappe, Phys. Rev. Lett. **109**, 116601 (2012).

[6] P. Král, J. Phys. Condens. Matter **12**, 4851 (2000).

[7] L. Braun, G. Mussler, A. Hruban, M. Konczykowski, T. Schumann, M. Wolf, M. Münzenberg, L. Perfetti, and T. Kampfrath, Nat. Commun. **7**, 13259 (2016).

[8] X. C. Zhang, J. T. Darrow, B. B. Hu, D. H. Auston, M. T. Schmidt, P. Tham, and E. S. Yang, *Appl. Phys. Lett.* **56**, 2228 (1990).

[9] P. C. Planken, M. C. Nuss, I. Brener, K. W. Goossen, M. S. Luo, S. L. Chuang, and L. Pfeiffer, *Phys. Rev. Lett.* **69**, 3800 (1992).

[10] J. M. Schleicher, M. H. Shayne, and A. C. A. Schmuttenmaer, *Jour. Appl. Phys.* **105**, 113116 (2009).

[11] K. Kushnir, M. Wang, P. D. Fitzgerald, K. J. Koski, and L. V. Titova, *ACS Energy Lett.* **2**, 1429 (2017).

[12] M. Sotome, M. Nakamura, J. Fujioka, M. Ogino, Y. Kaneko, T. Morimoto, Y. Zhang, M. Kawasaki, N. Nagaosa, Y. Tokura, and N. Ogawa, Proc. Natl. Acad. Sci. **116,** 1929 (2019).

[13] M. Sotome, M. Nakamura, Fujioka, M. Ogino, Y. Kaneko, T. Morimoto, Y. Zhang, M. Kawasaki, N. Nagaosa, Y. Tokura and N. Ogawa, Appl. Phys. Lett. **114**, 151101 (2019).

[14] N. Sirica, R. I. Tobey, L. X. Zhao, G. F. Chen, B. Xu, R. Yang, B. Shen, D. A. Yarotski, P. Bowlan, S. A. Trugman, J.-X. Zhu, Y. M. Dai, A. K. Azad, N. Ni, X. G. Qiu, A. J. Taylor, and R. P. Prasankumar, Phys. Rev. Lett. **122**, 197401 (2019).

[15] D. Rees, K. Manna, B. Lu, T. Morimoto, H. Borrmann, C. Felser, J. E. Moore, D. H. Torchinsky, and J. Orenstein, Sci. Adv. **6**, eaba0509 (2020).

[16] Z. Ni, K. Wang, Y. Zhang, O. Pozo, B. Xu, X. Han, K. Manna, J. Paglione, C. Felser, A. G. Grushin, F. de Juan, E. J. Mele, and L. Wu, arXiv:2006.09612 (2020).

[17] M. Bieler, K. Pierz, U. Siegner, and P. Dawson, Phys. Rev. B, **76**, 161304 (2007).

[18] S. Priyadarshi, M. Leidinger, K. Pierz, A. M. Racu, U. Siegner, M. Bieler, and P. Dawson, Appl. Phys. Lett. **95**, 151110 (2009).

[19] J. J. Hopfield and D. G. Thomas, Physical Review **122**, 35 (1961).

[20] G. Winterling and E. S. Koteles, Solid State Commun. **23**, 95 (1977).

[21] J. Voigt, F. Spiegelberg, and M. Senoner, Phys. Status Solidi B **91**, 189 (1979).

[22] I. Broser and M. Rosenzmeig, Phys. Rev. B **22**, 2000 (1980).

[23] H. M. van Driel and J. E. Sipe, "Cohrerent control of photocurrents in semiconductors", *Ultrafast Phenomena in Semiconductors*, chapter 5, pp261-306 (2001).

[24] N. Laman, M. Bieler, and H. M. van Driel, J. Appl. Phys. **98**, 103507 (2005).

[25] Q. Wu Q and X. C. Zhang, Appl. Phys. Lett. **68**, 1604 (1996).

[26] See Supplemental Material in *URL* for details of experiments and calculations. Their

references are following: Refs. 4, 24, 27-38.

[27] J. P. Perdew, K. Burke, and M. Ernzerhof, Phys. Rev. Lett. **77**, 3865 (1996).

[28] P. Giannozzi *et al*., J. Phys.: Condens. Matter **29**, 465901 (2017).

[29] D. R. Hamann, Phys. Rev. B **88**, 085117 (2013).

[31] J. Ibanez-Azpiroz, S. S. Tsirkin and I. Souza, Phys. Rev. B **97**, 245143 (2018).

[32] A. A. Mostofi, J. R. Yates, G. Pizzi, Y.-S. Lee, I. Souza, D. Vanderbilt and N. Marzari, Comput. Phys. Commun. **185**, 2309 (2014).

[33] J. L. P. Hughes and J. E. Sipe, Phys. Rev. B **53**, 10751 (1996).

[30] F. Nastos and J. E. Sipe, Phys. Rev. B **82**, 235204 (2010).

[34] R. W. Boyd, *Nonlinear optics*, (3rd edition), p48. Elsevier (2003).

[35] I. M. Catalano, A. Cingolani, C. Arnone, and S. Riva-Sanseverino, Solid State Commun., **49**, 1139 (1984).

[36] M. Bass, P. A. Franken, and J. F. Ward, Phys. Rev. **138**, A534 (1965)

[37] M. S. Dresselhaus, Solid State Physics, Part II: Optical Properties of Solids, Lecture Notes (Massachusetts Institute of Technology, Cambridge, MA, 2001), p.34. http://web.mit.edu/course/6/6.732/www/6.732-pt2.pdf (download in 2020/8)

[38] L. Ward, "Cadmium sulphide (CdS)." *Handbook of Optical Constants of Solids*. Academic Press, pp579-595 (1997).

[39] G. Blattner, G. Kurtze, G. Schmieder, and C. Klingshirn, Phys. Rev. B **25**, 7413 (1982).

[40] J. Conradi and R. R. Haering., Phys. Rev. **185**, 1088 (1969)

[41] W. C. Tait and R. L. Weiher, Physical Review **166**, 769 (1968)

[42] Y. S. Park and D. C. Reynolds, Phys. Rev. **132**, 2450 (1963)

[43] K. J. Hong, T. S. Jeong, C. J. Yoon, and Y. J. Shin, Journal of crystal growth, **218**, 19

(2000).

[44] D. Côté, N. Laman, and H. M. van Driel, Appl. Phys. Lett. **80**, 905 (2002).

[45] C. M. Bishop. *Pattern Recognition and Machine Learning* (Springer-Verlag New York, 2006).

[46] C. A. Stedmon and R. Bro, Limnol. Oceanogr. Methods **6**, 572 (2008).

[47] M. Dagenais and W. F. Sharfin, Phys. Rev. Lett. **58**, 1776 (1987)

[48] A. Imada, S. Ozaki, and S. Adachi, J. Appl. Phys. **92**, 1793 (2002).

[49] C. W. Litton, D. C. Reynolds, and T. C. Collins, Phys. Rev. B **6**, 2269 (1972).

[50] A. Bonnot, R. Planel, and C. Benoit à la Guillaume, Phys. Rev. B **9**, 690 (1974).

[51] L. Z. Tan, F. Zheng, S. M. Young, F. Wang, S. Liu, and A. M. Rappe, *npj Comput. Mater*. **2**, 1 (2016).

[52] W. Kraut and R. von Baltz, Phys. Rev. B 19, 1548 (1979).

[53] C. Somma, K. Reimann, C. Flytzanis, T. Elsaesser, and M. Woerner, Phys. Rev. Lett. **112**, 146602 (2014).

[54] A. Ghalgaoui, K. Reimann, M. Woerner, T. Elsaesser, C. Flytzanis, and K. Biermann, "Resonant second-order nonlinear terahertz response of gallium arsenide", Phys. Rev. Lett. **121**, 266602 (2018).

[55] K. H. Pantke and I. Broser, Phys. Rev. B **48**, 11752 (1993).

[56] C. Weisbuch and R. G. Ulbrich, in *Light Scattering in Solids III*, edited by M. Cardona and G. Guntherodt (Springer- Verlag, Berlin, 1978), p.207.

[57]T. Morimoto and N.Nagaosa, Sci. Adv. **2**, e1501524 (2016).

[58] F. Ruf, A. Magin, M. Schultes, E. Ahlswede, H. Kalt, and M. Hetterich, Appl. Phys. Lett. **112**, 083902 (2018).

Figures

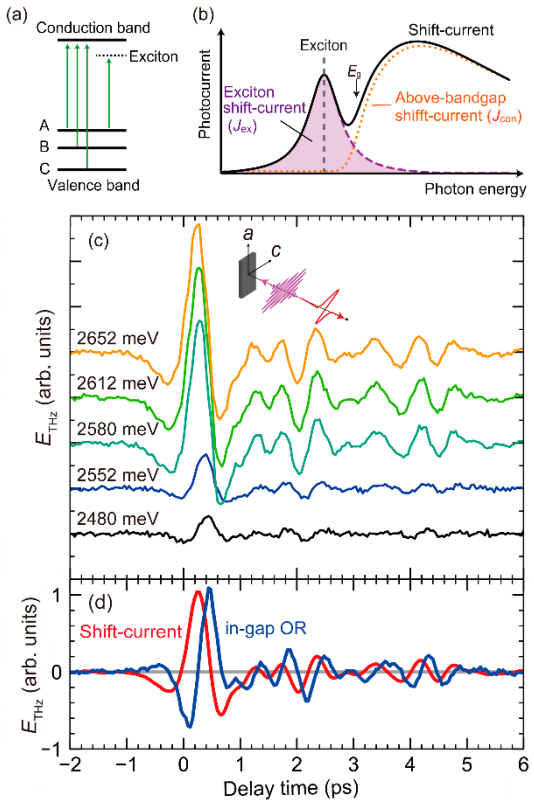

Fig. 1. (a, b) Schematics of exciton energy levels and shift-current spectra for CdS. Exciton shift-current is expected to appear at the exciton resonance, while total photocurrent is the sum of exciton shift-current and above-bandgap one. The spectra in (b) are based on Eqs. (1) and (2) in the main text. (c) Incident photon energy dependence of the terahertz emission near the A-exciton resonance (2552 meV) in CdS $(1\bar{1}00)$ ($E_{\mathrm{laser}} \parallel E_{\mathrm{THz}} \parallel c$, 1 μJ/pulse, offset for clarity). (d) Result of factor analysis separating contributions from exciton shift-current and in-gap optical rectification (in-gap OR).

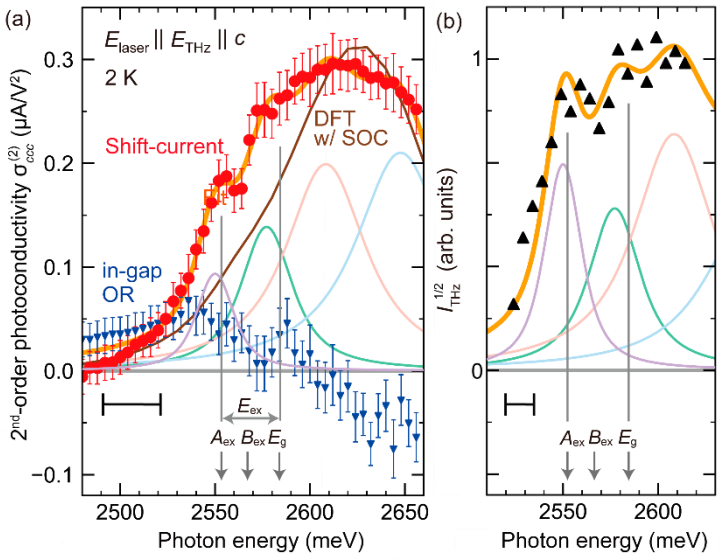

Fig. 2. (a) Excitation spectra of the 2nd-order photoconductivity for shift-current and in-gap optical rectification (in-gap OR). The shift-current component is fitted by the exciton and three above-bandgap resonances (with light colors). Theoretical spectrum for J_{con}(above-bandgap shift current) calculated with spin-orbit interaction is also plotted in brown. The onset energy is shifted to match with the band edge. Note that the excitonic effect is not taken into account, thus not reproducing the spectrum around the exciton resonance. DFT w/ SOC: density functional theory with spin-orbit coupling. (b) Excitation spectrum of the terahertz amplitude measured by the narrow-band laser source. The horizontal black bars in (a) and (b) indicate the experimental energy resolution (FWHM of the incident optical pulse energy). Exciton resonances, binding energy E_{ex} and bandgap E_{g} (grey arrows) are from Ref. 2339. The slight discrepancy between these literature values and the fitting peaks may be ascribed to the sample variation.

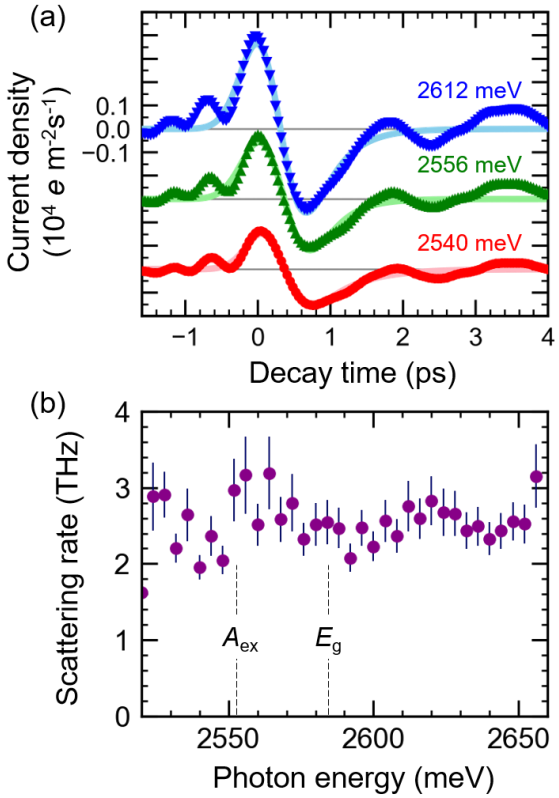

Fig.3. (a) Shift-current dynamics at 2540, 2556, and 2612 meV excitation ($E_{\mathrm{laser}} \parallel E_{\mathrm{THz}} \parallel c$, and T=2 K) (offset for clarity). (b) Incident photon energy dependence of the scattering rate.

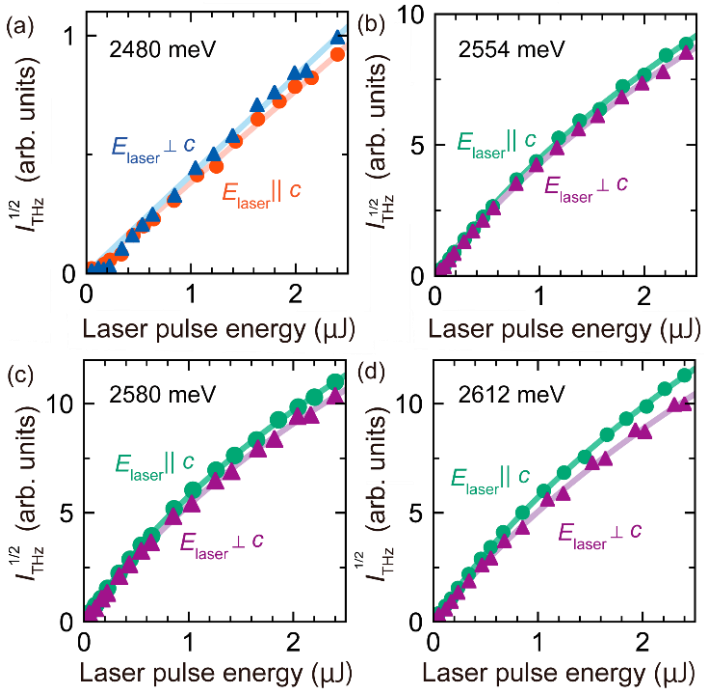

Fig. 4. Incident laser power dependences of the THz amplitude near the exciton resonance energies; (a) below and (b) at the exciton resonance, and (c),(d) above the exciton resonance. Fitting curves are from eq. (5), indicating a sublinear increase of THz amplitude on the incident pulse energy.